Exploring Synthetic Routes to Heteroleptic UIII, UIV and ThIV Bulky Bis(silyl)amide Complexes

DOI:
10.1002/ejic.201800036

Document Version
Accepted author manuscript

Citation for published version (APA):
Goodwin, C., Tuna, F., Mcinnes, E., & Mills, D. (2018). Exploring Synthetic Routes to Heteroleptic U^{III}, U^{IV} and Th^{IV} Bulky Bis(silyl)amide Complexes. *European Journal of Inorganic Chemistry*, (20-21). https://doi.org/10.1002/ejic.201800036

Published in:
European Journal of Inorganic Chemistry

EurJIC
European Journal of Inorganic Chemistry

A Journal of ChemPubSoc Europe

Accepted Article

Title: Exploring Synthetic Routes to Heteroleptic UIII, UIV and ThIV Bulky Bis(silyl)amide Complexes

Authors: Conrad Goodwin, Floriana Tuna, Eric McInnes, and David Paul Mills

To be cited as: *Eur. J. Inorg. Chem.* 10.1002/ejic.201800036

Link to VoR: http://dx.doi.org/10.1002/ejic.201800036

WILEY-VCH

10.1002/ejic.201800036

Exploring Synthetic Routes to Heteroleptic U^{III}, U^{IV} and Th^{IV} Bulky Bis(silyl)amide Complexes

Conrad A. P. Goodwin,[a] Floriana Tuna,[a] Eric J. L. McInnes,[a] and David P. Mills*[a]

Abstract: The bis(silyl)amide $\{N(SiMe_3)_2\}$ (N″) has supported spectacular actinide (An) chemistry for over 40 years, yet surprisingly there are only a handful of An complexes containing larger bis(silyl)amides, e.g. $[U(N^{**})_3]$ [N** = $\{N(SiMe_2tBu)_2\}$, **1**]. Herein we report the structural characterization of the U^{III} complexes $[U(N^{**})_2(\mu\text{-}I)]_2$ (**2**), $[U(N^{\dagger\prime})_2(\mu\text{-}I)]_2$ [N$^{\dagger\prime}$ = $\{N(SiiPr_3)(SiMe_3)\}$, **3**], $[U(N^{\dagger\dagger})(I)_2(THF)_2]$ [N†† = $\{N(SiiPr_3)_2\}$, **4**], $[U(N^{\dagger\dagger})_2(I)]$ (**5**), and $[U(N^{\dagger\prime})_2(I)(THF)]$ (**6**), and the An^{IV} complexes $[An(N^{**})\{N(SiMe_2tBu)(SiMetBuCH_2\text{-}\kappa^2\text{-}N,C)\}(\mu\text{-}Cl)]_2$ (**7-An**, An = U, Th) and $[Th(N^{**})_2\{N(SiMe_2tBu)(SiMetBuCH_2\text{-}\kappa^2\text{-}N,C)\}]$ (**8**). Low crystalline yields were obtained in all cases, presumably due to facile cyclometallation. Although this precluded full characterization of U^{III} **4** and **6**, and An^{IV} **7**-**8**, in the case of U^{III} **2**, **3** and **5** yields were high enough to perform NMR, EPR, NIR/UV/Vis and FTIR spectroscopy, elemental analysis and magnetic measurements.

Introduction

Bulky monodentate ligands are frequently used to stabilize low-coordinate metal complexes, which can exhibit interesting physicochemical properties as a result of their coordinative unsaturation [1]. Amides, NR_2, have found widespread application as their steric and electronic properties are readily tuned; bis(silyl)amides, $N(SiR_3)_2$, form an important subclass as the polarizable Si atoms produce softer, more charge-diffuse N-donors with distinctive electronic properties [2]. However, bis(silyl)amides are still relatively hard, thus they are well-suited to f-block chemistry [3], where bonding regimes are predominantly electrostatic [4]. Focusing on the actinides (An), hexamethyldisilazide (HMDS, $\{N(SiMe_3)_2\}$, N″) is the most frequently utilized bis(silyl)amide ligand and has stabilized numerous landmark compounds since the first example $[Th(N'')_3(Cl)]$ was reported by Bradley *et al*. in 1974 [5]. Of most relevance here, trigonal pyramidal $[U(N'')_3]$ provided the first example of a 3-coordinate An complex in 1979 [6], and this has been a vital starting material for the expansion of molecular U^{III} chemistry in the interim [7,8]. Given the importance of $[U(N'')_3]$, it is somewhat surprising that until 2014 only one An complex containing a bulkier monodentate bis(silyl)amide than N″, $[U^{III}\{N(SiPhMe_2)_2\}_3]$, had been isolated [9].

Recently, we developed synthetic routes to a series of bulky bis(silyl)amides and we have used these to stabilize low-coordinate f-element complexes [10]. The homoleptic U^{III} complex, $[U(N^{**})_3]$ [N** = $\{N(SiMe_2tBu)_2\}$, **1**], was the first structurally characterized trigonal planar An complex [10a]. Inspired by the paucity of bulky bis(silyl)amide An complexes and the interesting structure of **1**, we targeted related examples. Our results are reported herein.

Results and Discussion

We first attempted the synthesis of heteroleptic U^{IV} complexes by the chemical oxidation of **1**, as this had proved fruitful when using $[U(N'')_3]$ as a starting material [7,8]. However, we found that **1** does not react with 1 atm CO or CO_2, and an intractable mixture of products was obtained from the reaction of **1** with P_4. The diminished reactivity between **1** and CO or CO_2 contrasts with $[U(N'')_3]$, which reacts readily with these substrates [11,12]; we attribute this divergence to the increased kinetic stabilization provided by the bulkier N** ligands and the lack of a permanent electronic dipole in planar **1** [10a], though we note that further reactivity studies would be required to test this hypothesis. Given that U^{II} complexes have recently been synthesized by KC_8 reduction of U^{III} precursors [13-15], we treated diethyl ether suspensions of **1** with KC_8 in the presence of 18-crown-6 or 2.2.2-cryptand at –78 °C. Despite repeated attempts only intractable mixtures of products were obtained.

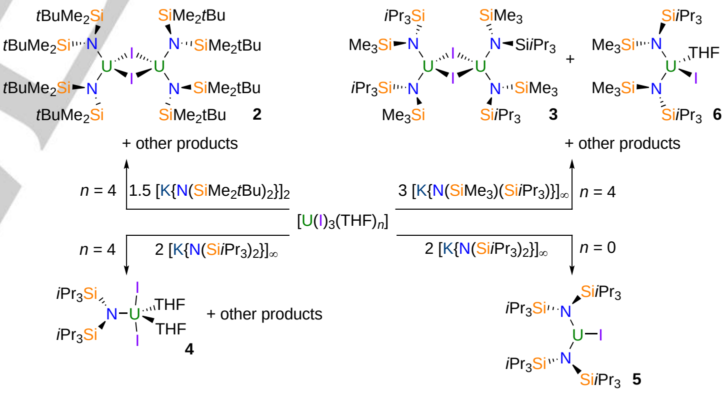

Scheme 1. Synthesis of **2**-**6**.

As initial reactivity studies of **1** were unproductive, we targeted novel bulky bis(silyl)amide U^{III} complexes. The separate reactions of $[UI_3(THF)_4]$ [16] with 1.5 eq. of $[\{K(\mu\text{-}N^{**})\}_2]_\infty$ [10a], 3 eq. of $[\{K(\mu\text{-}N^{\dagger\prime})\}_2]_\infty$ [N$^{\dagger\prime}$ = $\{N(SiiPr_3)(SiMe_3)\}$] [10c] and 2 eq. of $[\{K(N^{\dagger\dagger})\}_2]_\infty$ [N†† = $\{N(SiiPr_3)_2\}$] [10b] in THF gave the heteroleptic U^{III} complexes $[U(N^{**})_2(\mu\text{-}I)]_2$ (**2**), $[U(N^{\dagger\prime})_2(\mu\text{-}I)]_2$ (**3**) and $[U(N^{\dagger\dagger})(I)_2(THF)_2]$ (**4**), respectively (Scheme 1). It is noteworthy that **2** was isolated from an attempt to synthesize **1** on a large scale; the synthesis of **1** from $[UI_3(THF)_4]$ with 1.5 eq. of $[\{K(\mu\text{-}N^{**})\}_2]_\infty$ has previously been reported [10a].

---

[a] Dr C. A. P. Goodwin, Dr F. Tuna, Prof. E. J. L. McInnes, Dr D. P. Mills
School of Chemistry, The University of Manchester, Manchester, M13 9PL (UK)
E-mail: david.mills@manchester.ac.uk
https://www.research.manchester.ac.uk/portal/david.mills.html

Supporting information for this article is given via a link at the end of the document.

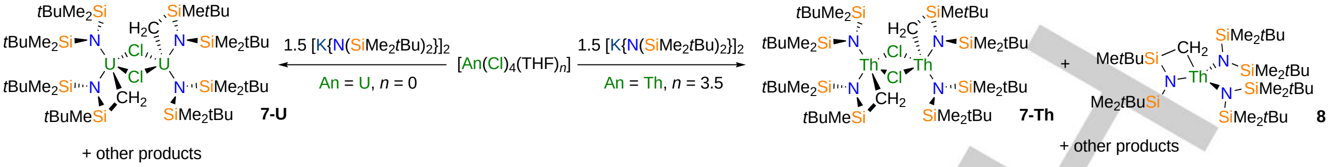

Scheme 2. Synthesis of **7**-**8**.

No homoleptic complexes were isolated, despite the stoichiometries employed, which we attribute to steric hindrance. Given that only monosubstitution was seen for $N^{\dagger\dagger}$ under these conditions, we performed the reaction of solvent-free UI_3 [16] with 1.5 eq. $[\{K(N^{\dagger\dagger})\}_2]_\infty$ in benzene, and we obtained the disubstituted complex $[U(N^{\dagger\dagger})_2(I)]$ (**5**). During the isolation of **3** crystals of the solvated monomer $[U(N^{\dagger\prime})_2(I)(THF)]$ (**6**) were identified by X-ray diffraction (XRD) (see below). No further characterization data could be obtained for **4** or **6**; in the case of **4** this was due to crystals forming together with an intractable purple oil, whilst a low yield was obtained for **6** (<1 %). Microanalysis results were obtained for **2**, **3** and **5**; although low carbon values were obtained reproducibly for **2** and **5** we have observed this phenomenon regularly for complexes of these ligands [10], thus **2**, **3** and **5** were characterized further [17].

The crystalline yields of **2**, **3** and **5** were uniformly poor (<10 %), which is in line with the 14 % yield reported for $[U(N'')_2(\mu\text{-}I)(THF)]_2$ [18]. It is noteworthy that the reported isolated yield of homoleptic **1** (62 %) [10a] is much higher than heteroleptic **2**, **3** and **5**. Ligand scrambling processes and cyclometallation are well-documented side-reactions in f-element bis(silyl)amide chemistry [1-3]. Although such processes cannot be discounted here, no other crystalline products could be isolated from the reaction mixtures of **2**, **3** and **5** to confirm these suppositions. The synthetic utility of a heteroleptic U^{III} halide complex in the preparation of a heterobimetallic complex containing a novel U^{III}-Fe^{II} bond has recently been demonstrated [19], but we have not investigated the further chemistry of **2**, **3** and **5** to date.

With heteroleptic U^{III} complexes in hand, we turned our attention to the synthesis of heteroleptic An^{IV} complexes. The separate reactions of UCl_4 [20] and $[ThCl_4(THF)_{3.5}]$ [21] with 1.5 or 2 eq. of dimeric $[\{K(\mu\text{-}N^{**})\}_2]_\infty$ in THF gave complex mixtures of products, from which crystals of the cyclometallated complexes $[An(N^{**})\{N(SiMe_2tBu)(SiMetBuCH_2\text{-}\kappa^2\text{-}N,C)\}(\mu\text{-}Cl)]_2$ (**7-An**, An = U, Th) and $[Th(N^{**})_2\{N(SiMe_2tBu)(SiMetBuCH_2\text{-}\kappa^2\text{-}N,C)\}]$ (**8**) were identified by single crystal XRD (Scheme 2). Despite exhaustive attempts we could not isolate appreciable quantities of **7-U**, **7-Th** or **8**, and crystals always formed along with numerous amorphous byproducts, thus no further characterization data could be obtained. It is noteworthy that the synthesis of $[An(N'')_3Cl]$ (An = Th [5, 22], U [22a,23]) by analogous routes is relatively straightforward. Thus, we postulate that the bulkier N** ligand hinders the third substitution; the Lewis acidic An^{IV} centers in the disubstituted intermediates then promote deprotonation of one of the coordinated N** ligands by basic KN**, leading to cyclometallation. Similar complexes have previously been synthesized in An^{IV} N″ chemistry, such as $[An(N'')_2\{N(SiMe_3)(SiMe_2CH_2\text{-}\kappa^2\text{-}N,C)\}]$ (An = Th, U) [24], and $[An(N'')\{N(SiMe_3)(SiMe_2CH_2\text{-}\kappa^2\text{-}N,C)\}_2]^-$ (An = Th, U) [25]; unlike the N** complexes **7**-**8** the N″ cyclometallates have been made deliberately in higher yields, thus their further chemistry has been investigated [3].

The ^1H NMR spectra of **2**, **3** and **5** all exhibit broad signals for silyl group protons. For **2** there are only two proton environments, for the Me and *t*Bu groups, but for **3** and **5** more complex spectra result. The presence of multiple methyl and methine resonances for **3** and **5** presumably arises from electrostatic contacts between some of these groups and U^{III} centers observed in the solid state that are maintained in solution (see below). We have observed such features previously for coordinatively saturated f-element complexes containing bulky bis(silyl)amides [10]. Only diamagnetic impurities were observed in the $^{13}C\{^1H\}$ NMR spectra of **2**, **3** and **5**, due to paramagnetic broadening. No signals were observed between +300 and –500 ppm in the $^{29}Si\{^1H\}$ NMR spectra of **2** and **3**, though a signal was observed at δ_{Si} = –264.1 ppm for **5** that is comparable to the signal previously seen for **1** (δ_{Si}: –296.0) [10a].

The UV/Vis/NIR spectra of **2**, **3** and **5** (Figure 1) are predominated by intense absorptions in the visible region, which we attribute to U^{III} $5f^3 \rightarrow 5f^2 6d^1$ transitions [26], and intense charge transfer bands $\tilde{\nu}$ >25,000 cm^{-1}. For monomeric **5**, maxima were observed at 18,200 (ε = 1,000 M^{-1} cm^{-1}) and 21,500 cm^{-1} (ε = 980 M^{-1} cm^{-1}). These bands have comparable intensities to those previously observed for **1** [$\tilde{\nu}/cm^{-1}$ (ε/M^{-1} cm^{-1}): 20,000 (776) and 22,500 (770)] [10a], though the substitution of a bis(silyl)amide ligand for an iodide has caused a bathochromic shift. Dimeric **2** and **3** exhibit similar energy absorptions that are approximately twice the intensity of **1** and **5** due to the presence of two U^{III} centers in these complexes [v'/cm^{-1} (ε/M^{-1} cm^{-1}): **2**: 19,200 (2,700) and 22,800 (2,000); **3**: 19,200 (2,200) and 22,200 (2,000), broad]. Parity-forbidden $5f \rightarrow 5f$ transitions are observed in the NIR region for **2**, **3** and **5**; for monomeric **5** the absorptions <9,000 cm^{-1} are generally weak (ε < 100 M^{-1} cm^{-1}) and comparable to those previously observed for **1**, and for dinuclear **3** the intensities of these absorptions correlate to two U^{III} centers (< 200 M^{-1} cm^{-1}). In contrast, the corresponding absorptions for **2** are far more intense (e.g. v = 8,300 cm^{-1}, ε = 500 M^{-1} cm^{-1}). We cannot explain the discrepancies between **2** and **3** given the similarity of their solid state structures (see below) but intense f-f transitions have previously been seen for uranium complexes and attributed to a 'charge-stealing' mechanism arising from the involvement of 5f orbitals in UV charge transfer bands [27].

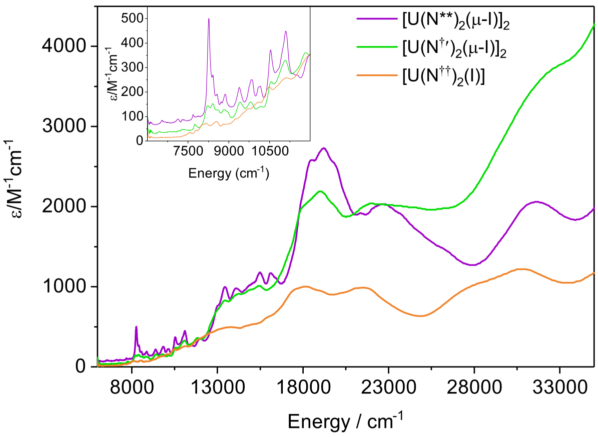

Figure 1. Electronic spectra of **2**, **3** and **5** (*ca.* 0.5 mM, 0.5 mM and 1.0 mM respectively in toluene, between 6,000–34,000 cm^{-1} (1,667–294 nm).

The molecular structures of **2**-**8** were determined by single crystal X-ray diffraction (**2**-**6**, **7-U** and **8** are depicted in Figures 2-8; see Supporting Information for the structure of **7-Th** and selected bond distances and angles compiled in Table S4). Dimeric **2** and **3** exhibit similar bulk features in the solid state, with the 4-coordinate U centers each bearing two N and two I donors; these structures are comparable to the La^{III} complex $[La\{N(Si\textit{t}BuMe_2)(SiMe_3)\}_2(\mu\text{-}I)]_2$ [10b]. The steric requirements of N** and $N^{\dagger\prime}$ are evidenced by the N–U–N angles being >119° in both complexes. The mean U–N bond distances in **2** [2.357(4) Å] and **3** [2.336(4) Å] are shorter than previously seen for **1** [2.409(7) Å mean] [10a] due to the absence of a third bulky ligand, and are longer than those seen for 5-coordinate dinuclear $[U(N'')_2(\mu\text{-}I)(THF)]_2$ [2.314(4) Å] [18], which contains coordinated THF as N″ is smaller than N** and $N^{\dagger\prime}$. The coordinative unsaturation in **2** and **3** produces a number of electrostatic contacts between U and methyl/methine groups; the resultant U···C distances <3.2 Å for all complexes are included in Table S4.

Complexes **4**-**6** are monomeric in the solid state and their coordination numbers vary according to the steric influence of bound bis(silyl)amides: 5-coordinate **4** contains one $N^{\dagger\dagger}$, two iodides and two THF molecules, **6** is 4-coordinate with two $N^{\dagger\prime}$, one iodide and one THF, and **5** is 3-coordinate with two $N^{\dagger\dagger}$ and one iodide. The metrical parameters of **4** and **6** are unremarkable, but the presence of two bulky $N^{\dagger\dagger}$ ligands in **5** engender a relatively long U–N bond [2.388(11) Å] and large N–U–N angle [134.6(6)°]. This results in a Y-shaped coordination geometry with the U center within the N_2I plane. Although no U···C distances <3.2 Å are seen for **5**, two methine groups oriented above and below the UN_2I plane lead to two short U···H electrostatic contacts [2.573 Å]; similar features were previously observed for **1** [10a].

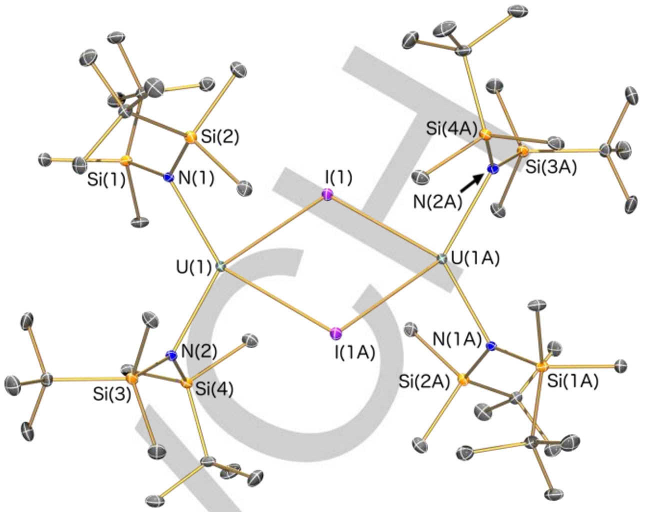

Figure 2. Molecular structure of **2** with selected atom labelling. Displacement ellipsoids set at the 40 % probability level, and H atoms are removed for clarity.

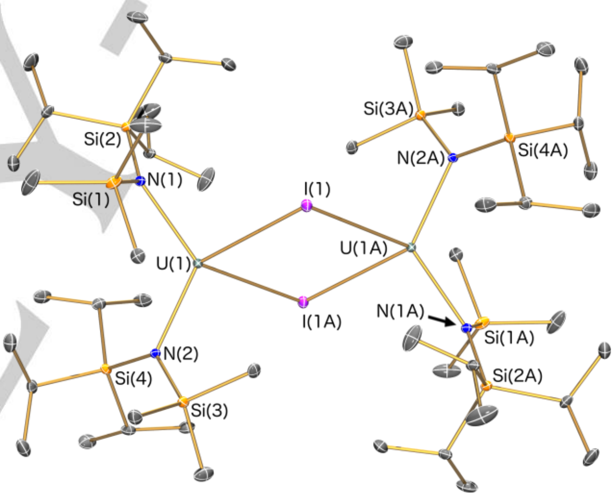

Figure 3. Molecular structure of **3** with selected atom labelling. Displacement ellipsoids set at the 40 % probability level, and H atoms are removed for clarity.

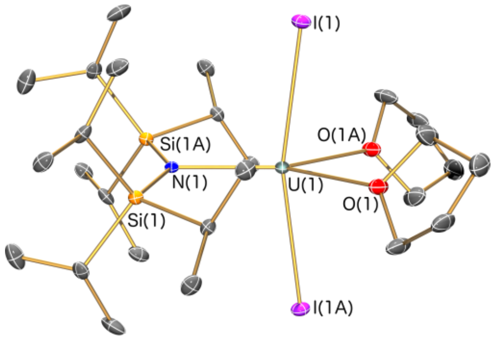

Figure 4. Molecular structure of **4** with selected atom labelling. Displacement ellipsoids set at the 40 % probability level, and H atoms are removed for clarity.

10.1002/ejic.201800036

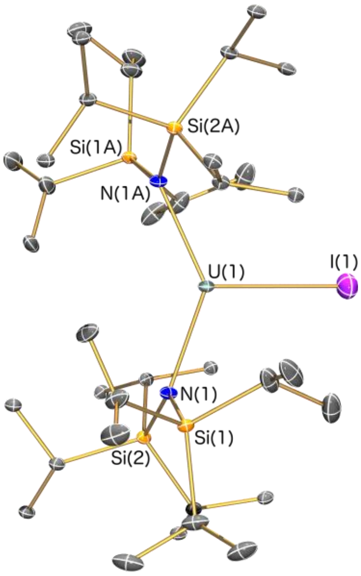

Figure 5. Molecular structure of **5** with selected atom labelling. Displacement ellipsoids set at the 40 % probability level, and H atoms are removed for clarity.

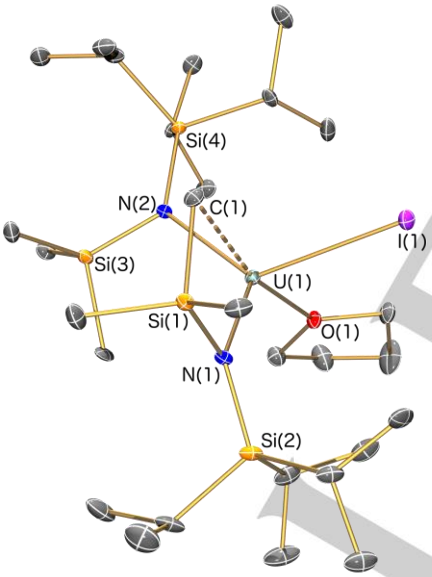

Figure 6. Molecular structure of **6** with selected atom labelling. Displacement ellipsoids set at the 40 % probability level, and H atoms are removed for clarity.

The cyclometallated dinuclear complexes **7-An** are structurally analogous, hence these are discussed together. The formally 5-coordinate An centers are bridged by two chlorides, and each contain one bidentate {N(SiMe$_2$*t*Bu)(SiMe*t*BuCH$_2$-κ^2-*N*,*C*)} and one N**. The similarity of the cyclometallated ligand with N** leads to significant crystallographic disorder so they cannot be easily distinguished; this results in a wide range of An–N and An–C distances, hence we do not discuss the metrical parameters of the 4-membered metallacycles. We previously observed this phenomenon for the related Yb^{III} cyclometallate [Yb(N**){N(Si*t*BuMe$_2$)(Si*t*BuMeCH$_2$)}(THF)]] [10e]. Formally 4-coordinate **8** is similarly disordered; in addition to the N** and cyclometallated ligands the Th^{IV} center is disordered above and below the N$_3$ plane by 0.2666(7) Å. The structure of **8** is reminiscent of [K(DME)][Th(N″){N(SiMe$_3$)(SiMe$_2$CH$_2$-κ^2-*N*,*C*)}$_2$] [25c], and the bond lengths/angles are comparable, so we do not comment on this further.

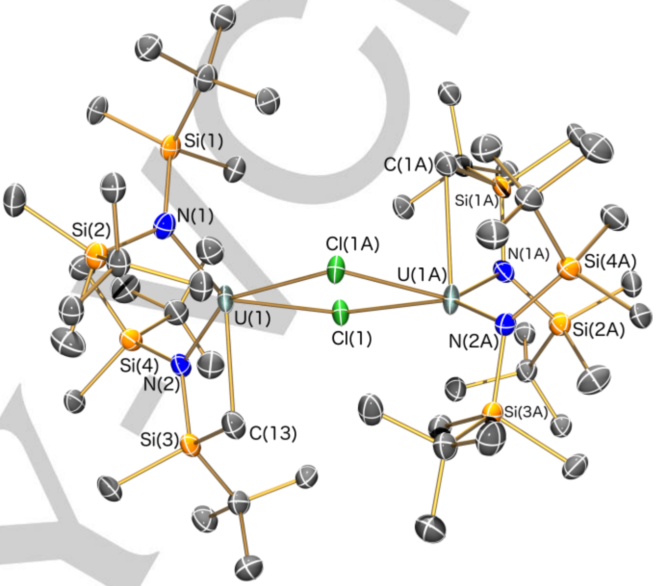

Figure 7. Molecular structure of **7-U** with selected atom labelling (**7-Th** is structurally analogous). Displacement ellipsoids set at the 40 % probability level, and H atoms are removed for clarity.

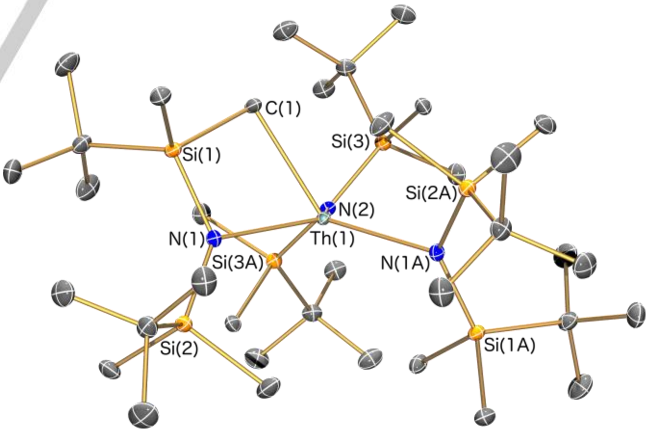

Figure 8. Molecular structure of **8** with selected atom labelling. Displacement ellipsoids set at the 40 % probability level, and H atoms are removed for clarity.

The solution magnetic moments of **2** (1.80 cm^3 K mol^{-1}), **3** (2.19 cm^3 K mol^{-1}) and **5** (1.13 cm^3 K mol^{-1}) were determined at 298 K in [D$_6$]benzene using the Evans method [28]. Variable temperature magnetic measurements were performed on powdered samples of **2**, **3** and **5** suspended in eicosane; at 300

K magnetic susceptibility temperature products, χT, of 2.07, 2.04 and 0.98 cm^3 K mol^{-1} were respectively obtained, which considering weighing errors and diamagnetic corrections are in good agreement with solution moments. The χT value of **5** at 298 K is comparable to that previously observed for **1** (1.07 cm^3 K mol^{-1}) [10a]; at this temperature thermal population of all crystal field states is incomplete [29], thus this value is lower than predicted for a free-ion 5f^3 $^4I_{9/2}$ ground state (1.70 cm^3 K mol^{-1}), but is around the middle of the reported range for monometallic U^{III} complexes (0.38–1.81 cm^3 K mol^{-1}) [30]. The χT values of **2** and **3** at 298 K are higher than the reported range for dinuclear U^{III} complexes (0.28–1.53 cm^3 K mol^{-1}), but are approximately double the value for the monomer **5**.

The χT for **5** decreases only slowly on cooling, reaching 0.76 cm^3 K mol^{-1} at 2 K; a notably weaker temperature dependence than for **1** (which varies from 1.07 to 0.41 cm^3 K mol^{-1} in the same temperature range). This higher low temperature limit for **5** suggests a more magnetic ground state, and this is consistent with the low temperature EPR spectrum (Figure S17) which shows resonances at g_{eff} = 4.9 and 3.3 (final g-value unobserved) in contrast with the g_{eff} = 3.55, 2.97 and 0.553 observed for **1** [10a]. The ground state of **1** is reasonably described by the $|m_J|$ = ½ Kramers doublet of the $^4I_{9/2}$ term, assuming a Russell-Saunders description, which is stabilized by the trigonal-planar crystal field with no axial ligands. The EPR spectrum of **5** implies a substantial contribution from a higher $|m_J|$ state in the ground doublet, and this would be consistent with the lower symmetry, and the weaker field of the iodide ligand, leading to the principal axis being rotated towards the coordination plane.

The $\chi T(T)$ product for **2** decreases to 0.16 cm^3 K mol^{-1} at 2 K, and a maximum is observed at 16 K in $\chi(T)$ (Figure 9(a)). These data are consistent with significant antiferromagnetic coupling between the U^{III} centers. Supporting this, **2** gives a very low magnetization (M, *ca.* 0.1 μ_B) at low fields before increasing rapidly above 6 T (Figure 9(b)), consistent with a field-induced level crossing of a magnetic excited state with a non- (or weakly-) magnetic ground state. The non-zero low-field magnetization is likely the result of a small quantity of a monomer impurity (which would not be readily detectable in elemental analysis or by NMR spectroscopy). Complex **3** also shows evidence for antiferromagnetic coupling in magnetization behavior (Figure S11), but there is a much more significant low-field step. We note that on one occasion crystals of **6** were identified during the crystallization of **3**, and analysis of the powder X-ray diffraction data of a sample of **3** (Figures S18-20) indicates significant contamination with complex **6** (the ratio of **3** to **6** is approximately 1:3). Hence, we refrain from discussing the data for **3** further.

For **5**, $M(H)$ saturates in relatively low applied magnetic field (H) as expected for a well isolated Kramers doublet (Figure 9(b)). In common with many U(III) monomers [31], complex **5** exhibits slow relaxation in ac magnetic measurements, with a peak in out-of-phase $\chi''(T)$ at low temperatures when a small dc field is applied, and this also manifests as an open hysteresis loop at 1.8 K. This behavior is similar to that of **1** [10a].

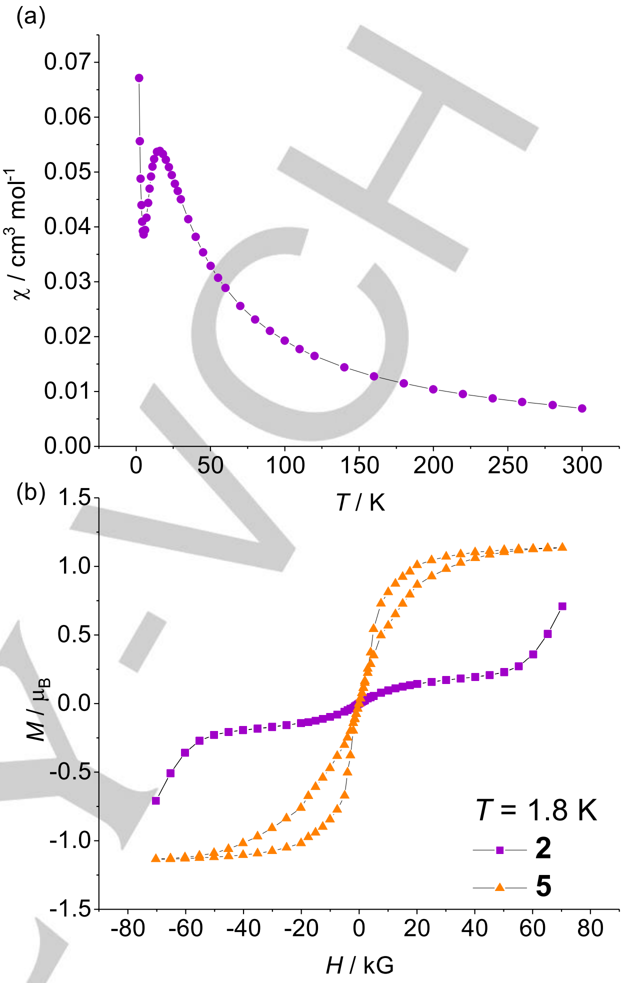

Figure 9. Selected magnetic susceptibility data: (a) magnetic susceptibility, χ (cm^3 mol^{-1}) for **2** in a 1 kG applied dc field; (b) magnetic hysteresis at 1.8 K for **2** and **5**, sweep rate 13 G s^{-1}.

Conclusions

Heteroleptic U^{III} complexes of the bulky bis(silyl)amides N**, N$^{\dagger\prime}$ and N†† can be prepared from UI$_3$ and potassium ligand transfer agents. The low isolated crystalline yields obtained are presumably due to sluggish ligand substitution and facile cyclometallation, which both result from the considerable steric bulk of these systems. These effects were magnified in the attempted synthesis of An^{IV} N** complexes as the Lewis acidic An^{IV} centers promote cyclometallation. Although homoleptic U^{III} complexes of N$^{\dagger\prime}$ and N†† were elusive, the isolation of [U(N††)$_2$(I)] is notable as a rare example of a heteroleptic 3-coordinate An complex. Given the sluggish reactivity of [U(N**)$_3$] observed herein, the presence of an ancillary halide ligand in [U(N††)$_2$(I)] provides an additional functionality to utilize in future studies of bulky bis(silyl)amide U^{III} chemistry.

Experimental Section

General

All manipulations were carried out using standard Schlenk techniques, or an Innovative Technology PureLab HE glovebox, under an atmosphere of dry argon. Solvents were dried by refluxing over potassium, or NaK (Et_2O) and degassed before use. All solvents were stored over potassium mirrors except for THF which was stored over activated 4 Å sieves. $[D_6]$benzene was distilled from potassium, degassed by three freeze-pump-thaw cycles and stored under argon. $[UI_3(THF)_4]$ [16], UI_3 [16], UCl_4 [20], $[ThCl_4(THF)_{3.5}]$ [21], **1** [10a], $[\{K(\mu\text{-}N^{**})\}_2]_\infty$ [10a], $[\{K(\mu\text{-}N^{\dagger\prime})\}_2]_\infty$ [10c] and $[\{K(N^{\dagger\dagger})\}_2]_\infty$ [10b] were synthesized according to published procedures. ^1H, ^{13}C and ^{29}Si NMR spectra were recorded on a Bruker DPX400 spectrometer operating at 400.2, 100.6 and 79.5 MHz respectively; chemical shifts are relative to TMS. FTIR spectra were recorded as Nujol mulls in KBr discs on a Perkin Elmer Spectrum RX1 spectrometer. UV-Vis-NIR spectroscopy was performed on samples in Youngs tap appended 10 mm pathlength quartz cuvettes on an Agilent Technologies Cary Series UV-Vis-NIR Spectrophotometer from 175–3300 nm. Elemental microanalyses were carried out by Mr Martin Jennings and Mrs Anne Davies at The University of Manchester School of Chemistry Microanalysis service. Q-band EPR spectroscopy was performed on powdered samples in sealed quartz tubes at 5 K. Magnetic measurements were made using a Quantum Design MPMS-XL7 SQUID magnetometer on ground crystalline samples suspended in eicosane in sealed borosilicate tubes.

Preparation of $[U(N^{**})_2(\mu\text{-}I)]_2$ (2)

THF (50 mL) was added to a pre-cooled (–78 °C) mixture of $[U(I)_3(THF)_4]$ (4.022 g, 4.43 mmol) and $[K\{N(SiMe_2\textit{t}Bu)_2\}]_2$ (3.647 g, 6.43 mmol). The reaction mixture was allowed to warm to room temperature slowly, and stirred for 16 hrs. Volatiles were removed from the purple slurry *in vacuo* and the resultant solids were extracted with toluene (50 mL). The red/purple solution was concentrated and stored at –25 °C for 24 hours to afford **2** (0.2666 g, 7 %) as purple/red blocks. Anal Calcd for $C_{48}H_{120}Si_8I_2N_4U_2(C_7H_8)$: C, 36.70; H, 7.17; N, 3.11. Found: C, 32.40; H, 6.87; N, 2.88. ^1H NMR (400.13 MHz, $[D_6]$benzene, 25 °C, TMS): δ = 3.75 (v½ ~ 250 Hz), 24 H; 8.65 (v½ ~ 800 Hz), 36 H. FTIR (Nujol) $\tilde{\nu}$: 1248 (m), 1011 (s), 990 (s), 937 (w), 830 (s), 806 (s), 785 (s), 766 (s), 747 (s), 658 (w), 650 (w) cm^{-1}.

Preparation of $[U(N^{\dagger\prime})_2(\mu\text{-}I)]_2$ (3) and $[U(N^{\dagger\prime})_2(I)(THF)]$ (6)

THF (30 mL) was added to a pre-cooled (–78 °C) mixture of $[U(I)_3(THF)_4]$ (1.361 g, 1.5 mmol) and $[K\{N(Si\textit{i}Pr_3)(SiMe_3)\}]$ (1.233 g, 4.35 mmol). The reaction mixture was allowed to warm to room temperature slowly, and stirred for 16 hrs. Volatiles were removed from the purple slurry *in vacuo* and the resultant solids were extracted with hexane (20 mL). The red/purple solution was concentrated, and upon standing at room temperature several red/purple needles of **6** formed. These were isolated and the mother liquor was stored at 4 °C for 24 hours to form purple needles of **3** (0.0763 g, 6 %). Anal Calcd for $C_{48}H_{120}Si_8I_2N_4U_2$: C, 33.75; H, 7.08; N, 3.28. Found: C, 33.64; H, 7.07; N, 3.54. ^1H NMR (400.13 MHz, $[D_6]$benzene, 25 °C, TMS): δ = –29.54 (v½ ~ 450 Hz), 6 H; –19.50 (v½ ~ 1,000 Hz), 6 H; –16.44 (v½ ~ 600 Hz), 6 H; –4.83 (v½ ~ 350 Hz), 24 H; 9.92 (v½ ~ 300 Hz), 18 H. FTIR (Nujol) $\tilde{\nu}$: 1250 (m), 993 (v. w), 943 (m), 882 (w), 839 (m), 820 (m), 756 (m), 739 (m), 672 (w), 653 (v. w) cm^{-1}.

Preparation of $[U(N^{\dagger\dagger})(I)_2(THF)_2]$ (4)

Benzene (30 mL) was added to a mixture of $[U(I)_3(THF)_4]$ (1.814 g, 2 mmol) and $[K\{N(Si\textit{i}Pr_3)_2\}]$ (1.471 g, 4 mmol) at room temperature. Over the course of several minutes, a blue solution developed, with blue precipitate, which adhered to the vessel walls. The mixture was stirred for 16 hours, after which a purple/brown solution with pale precipitate had developed. Volatiles were removed *in vacuo*, and the brown solid was extracted with diethyl ether (30 mL). The brown solution was filtered, concentrated to *ca*. 2 mL, and stored at –20 °C for 24 hours to afford purple needles of **4** as part of an oily purple intractable mixture.

Preparation of $[U(N^{\dagger\dagger})_2(I)]$ (5)

Toluene (40 mL) was added to a pre-cooled (–30 °C) mixture of UI_3 (1.856 g, 3 mmol) and $[K\{N(Si\textit{i}Pr_3)_2\}]$ (2.096 g, 5.7 mmol). The reaction mixture was stirred at –30 °C for 30 minutes and was then allowed to stir at room temperature for 16 hours. Volatiles were removed from the purple mixture *in vacuo*, and the tacky purple solid was triturated once with diethyl ether (40 mL), and then extracted with a second portion of diethyl ether (20 mL). The purple solution was filtered, concentrated to 2 mL and layered with pentane (2 mL). Storage of the mixture at –20 °C for 24 hours afforded **5** as purple blocks (0.2905 g, 10 %). Anal Calcd for $C_{36}H_{84}Si_4N_2UI$: C, 42.29; H, 8.28; N, 2.74. Found: C, 41.45; H, 8.58; N, 2.83. ^1H NMR (400.13 MHz, $[D_6]$benzene, 25 °C, TMS): δ = –36.20 (v½ ~ 600 Hz), 6 H; –3.75 (v½ ~ 350 Hz), 54 H; –2.46 (v½ ~ 600 Hz), 12 H. FTIR (Nujol) $\tilde{\nu}$: 1215 (v.w), 1117 (m), 1092 (br. m), 1069 (m), 958 (v. w), 944 (br. w), 882 (w), 694 (m), 652 (v. w) cm^{-1}.

Preparation of $[U(N^{**})\{N(SiMe_2tBu)(SiMetBuCH_2\text{-}\kappa^2\text{-}N,C)\}(\mu\text{-}Cl)]_2$ (7-U)

THF(20 mL) was added to a pre-cooled (–78 °C) mixture of UCl_4 (0.7597 g, 2 mmol) and $[Na\{N(SiMe_2\textit{t}Bu)_2\}]$ (1.605 g, 3 mmol). The resultant green/brown reaction mixture was warmed to room temperature and after 1 hour a white precipitate formed. The mixture was stirred for a further 16 hours, filtered, and volatiles were removed *in vacuo*. The brown solid was extracted with hexane (20 mL). Concentration of the brown solution to 4 mL afforded several brown needles of **7-U**, and an intractable oily red residue.

Preparation of $[Th(N^{**})\{N(SiMe_2tBu)(SiMetBuCH_2\text{-}\kappa^2\text{-}N,C)\}(\mu\text{-}Cl)]_2$ (7-Th) and $[Th(N^{**})_2\{N(SiMe_2tBu)(SiMetBuCH_2\text{-}\kappa^2\text{-}N,C)\}]$ (8)

Diethyl ether (20 mL) was added to a pre-cooled (–78 °C) mixture of $[Th(Cl)_4(THF)_{3.5}]$ (1.252 g, 2 mmol) and $[Na\{N(SiMe_2\textit{t}Bu)_2\}]$ (1.605 g, 6 mmol). The white slurry was allowed to warm to room temperature slowly, with slow dissolution of most of the solids, and the mixture was stirred for 16 hours. Volatiles were removed *in vacuo* and the tacky white solid was extracted with hexane (20 mL). Concentration of the hexane to 1 mL followed by storage at 4 °C afforded several crystals of **8**. Re-extraction of the hexane insoluble residue with toluene (10 mL) followed by evaporation of the volatiles *in vacuo* afforded a tacky white solid. This residue was then extracted with hot hexamethyldisiloxane (10 mL), concentrated to 3 mL and stored at 4 °C to afford a few crystals of **7-Th**.

Acknowledgements

We thank the EPSRC (Doctoral Prize Fellowship to C.A.P.G.) and The University of Manchester for funding this work. We also thank the EPSRC UK National Electron Paramagnetic Resonance Service for access to the EPR facility and the SQUID magnetometer. We thank Dr Fabrizio Ortu for assistance with single crystal XRD experiments, Dr Iñigo Vitorica-Yrezabal for assistance with powder XRD experiments, and Dr Nicholas Chilton for helpful discussions. Research data files supporting this publication are available from Mendeley Data at doi:10.17632/nc995wjbmm.1. CCDC 1813031–1813038 contain the supplementary crystal data for this article. These data can be obtained free of charge from the Cambridge Crystallographic Data Centre via www.ccdc.cam.ac.uk/data_request/cif.

Keywords: uranium • thorium • ligand design • ligand effects

[1] P. P. Power, *J. Organomet. Chem.* **2004**, *689*, 3904–3919.
[2] a) *Metal and Metalloid Amides* (Eds.: M. F. Lappert, P. P. Power, A. R. Sanger, R. C. Srivastava), Ellis Horwood-Wiley, Chichester, **1980**; b) R. Anwander, *Top. Curr. Chem.* **1996**, *179*, 33–112; c) *Metal Amide Chemistry* (Eds.: M. F. Lappert, A. Protchenko, P. P. Power, A. Seeber), Wiley, Chichester, **2008**.
[3] C. A. P. Goodwin, D. P. Mills, *Organomet. Chem.* **2017**, *41*, 123–156.
[4] a) *The Chemistry of the Actinide and Transactinide Elements* (Eds.: L. R. Morss, N. M. Edelstein, J. Fuger), Springer, Dordrecht, **2006**; b) *The Rare Earth Elements: Fundamentals and Applications* (Ed. D. A. Atwood), Wiley, Chichester, **2012**.
[5] D. C. Bradley, J. S. Ghotra, F. A. Hart, *Inorg. Nucl. Chem. Lett.* **1974**, *10*, 209–211.
[6] R. A. Andersen, *Inorg. Chem.* **1979**, *18*, 1507–1509.
[7] R. J. Baker, *Coord. Chem. Rev.* **2012**, *256*, 2843–2871.
[8] S. T. Liddle, *Angew. Chem. Int. Ed.* **2015**, *44*, 8604–8641.
[9] S. M. Mansell, B. F. Perandones, P. L. Arnold, *J. Organomet. Chem.* **2010**, *695*, 2814–2821.
[10] a) C. A. P. Goodwin, F. Tuna, E. J. L. McInnes, S. T. Liddle, J. McMaster, I. J. Vitorica-Yrezabal, D. P. Mills, *Chem. Eur. J.* **2014**, *20*, 14579–14583; b) C. A. P. Goodwin, K. C. Joslin, S. J. Lockyer, A. Formanuik, G. A. Morris, F. Ortu, I. J. Vitorica-Yrezabal, D. P. Mills, *Organometallics* **2015**, *34*, 2314–2325; c) N. F. Chilton, C. A. P. Goodwin, D. P. Mills, R. E. P. Winpenny, *Chem. Commun.* **2015**, *51*, 101–103; d) C. A. P. Goodwin, N. F. Chilton, G. F. Vettese, E. Moreno Pineda, I. F. Crowe, J. W. Ziller, R. E. P. Winpenny, W. J. Evans, D. P. Mills, *Inorg. Chem.* **2016**, *55*, 10057–10067; e) C. A. P. Goodwin, N. F. Chilton, L. S. Natrajan, M.-E. Boulon, J. W. Ziller, W. J. Evans, D. P. Mills, *Inorg. Chem.* **2017**, *56*, 5959–5970; f) F. Ortu, M. Gregson, A. J. Wooles, D. P. Mills, S. T. Liddle, *Organometallics*, **2017**, *36*, 4584–4590.
[11] P. L. Arnold, Z. R. Turner, R. M. Bellabarba, R. P. Tooze, *Chem. Sci.* **2011**, *2*, 77–79.
[12] S. M. Mansell, N. Kaltsoyannis, P. Arnold, *J. Am. Chem. Soc.* **2011**, *133*, 9036–9051.
[13] M. R. MacDonald, M. E. Fieser, J. E. Bates, J. W. Ziller, F. Furche, W. J. Evans, *J. Am. Chem. Soc.* **2013**, *135*, 13310–13313.
[14] H. S. La Pierre, A. Scheurer, F. W. Heinemann, W. Hieringer, K. Meyer, *Angew. Chem. Int. Ed.* **2014**, *53*, 7158–7162.
[15] C. J. Windorff, M. R. MacDonald, K. R. Meihaus, J. W. Ziller, J. R. Long, W. J. Evans, *Chem. Eur. J.* **2016**, *22*, 772–782.
[16] L. R. Avens, S. G. Bott, D. L. Clark, A. P. Sattelberger, J. G. Watkin, B. D. Zwick, *Inorg. Chem.* **1994**, *33*, 2248–2256.
[17] Full details can be found in the Supporting Information.
[18] S. M. Mansell, P. A. Arnold, *Polyhedron* **2016**, *116*, 82–87.
[19] S. Fortier, F. R. Aguilar-Calderón, B. Vlaisavljevich, A. J. Metta-Magaña, A. G. Goos, C. E. Botez, *Organometallics* **2017**, *36*, 4591–4599.
[20] a) D. Patel, A. J. Wooles, E. Hashem, H. Omorodion, R. J. Baker, S. T. Liddle, *New J. Chem.* **2015**, 39, 7559–7562; b) J. L. Kiplinger, D. E. Morris, B. L. Scott, C. J. Burns, *Organometallics* **2002**, *21*, 5978–5982.
[21] T. Cantat, B. L. Scott, J. L. Kiplinger, *Chem. Commun.* **2010**, *46*, 919–921.
[22] a) H. W. Turner, R. A. Andersen, A. Zalkin, D. H. Templeton, *Inorg. Chem.* **1979**, *18*, 1221–1224; b) D. E. Smiles, G. Wu, N. Kaltsoyannis, T. W. Hayton, *Chem. Sci.* **2015**, *6*, 3891–3899.
[23] A. Hervé, Y. Bouzidi, J.-C. Berthet, L. Belkhiri, P. Thuéry, A. Boucekkine, M. Ephritikhine, *Inorg. Chem.* **2015**, *54*, 2474–2490.
[24] a) A. Dormond, A. Aaliti, C. Moïse, *J. Org. Chem.* **1988**, *53*, 1034–1037; b) M. J. Monreal, R. K. Thomson, T. Cantat, N. E. Travia, B. L. Scott, J. L. Kiplinger, *Organometallics* **2011**, *30*, 2031–2038; c) S. J. Simpson, H. W. Turner, R. A. Andersen, *J. Am. Chem. Soc.* **1979**, *101*, 7728–7729; d) S. J. Simpson, H. W. Turner, R. A. Andersen, *Inorg. Chem.* **1981**, *20*, 2991–2995.
[25] a) O. Bénaud, J. C. Berthet, P. Thuéry, M. Ephritikhine, *Inorg. Chem.* **2010**, *49*, 8117–8130; b) I. Korobkov, S. Gambarotta, *Inorg. Chem.* **2010**, *49*, 3409–3418; c) N. L. Bell, L. Maron, P. L. Arnold, *J. Am. Chem. Soc.* **2015**, *137*, 10492–10495.
[26] W. T. Carnall, *J. Chem. Phys.* **1992**, *96*, 8713–8726.
[27] a) D. P. Mills, F. Moro, J. McMaster, J. van Slageren, W. Lewis, A. J. Blake, S. T. Liddle, *Nature Chem.* **2011**, *3*, 454–560; b) C. R. Graves, P. Yang, S. A. Kozimor, A. E. Vaughn, D. L. Clark, S. D. Conradson, E. J. Schelter, B. L. Scott, J. D. Thompson, P. J. Hay, D. E. Morris, J. L. Kiplinger, *J. Am. Chem. Soc.* **2008**, *130*, 5272–5285; c) D. E. Morris, R. E. Da Re, K. C. Jantunen, I. Castro-Rodriguez, J. L. Kiplinger, *Organometallics* **2004**, *23*, 5142–5153.
[28] S. K. Sur, *J. Magn. Reson.* **1989**, *82*, 169–173.
[29] E. R. Jones, M. E. Hendricks, J. A. Stone, D. G. Karraker *J. Chem. Phys.* **1974**, *60*, 2088–2094.
[30] D. R. Kindra, W. J. Evans, *Chem. Rev.* **2014**, *114*, 8865–8882.
[31] F. Moro, D. P. Mills, S. T. Liddle, J. van Slageren, *Angew. Chem. Int. Ed.* **2013**, *52*, 3430–3433.

Entry for the Table of Contents

FULL PAPER

Herein we report the synthesis and characterization of heteroleptic U^{III} bulky bis(silyl)amide complexes by salt metathesis methodologies, and explore the viability of similar synthetic routes to related U^{IV} and Th^{IV} bis(silyl)amide complexes.

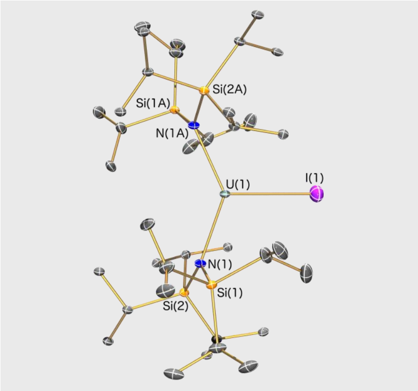

Actinide Bis(silyl)amides

*Conrad A. P. Goodwin, Floriana Tuna, Eric J. L. McInnes, and David P. Mills**

Page No. – Page No.

Exploring Synthetic Routes to Heteroleptic U^{III}, U^{IV} and Th^{IV} Bulky Bis(silyl)amide Complexes